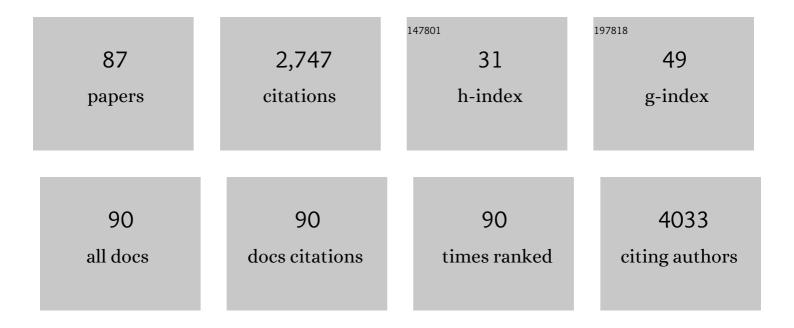
## Yueming Sun

List of Publications by Year in descending order

Source: https://exaly.com/author-pdf/6739650/publications.pdf Version: 2024-02-01



#	Article	IF	CITATIONS
1	Molecular core–shell structure design: Facilitating delayed fluorescence in aggregates toward highly efficient solutionâ€processed OLEDs. Aggregate, 2022, 3, .	9.9	33
2	Surfactantâ€Free and Microporous AlOOH/Al <sub>2</sub> O <sub>3</sub> Nanosheets on TiO <sub>2</sub> â€Based Nanofibers: A Sustainedâ€Release Dominated Topotactic Transformation. ChemNanoMat, 2022, 8, .	2.8	1
3	A periphery hindered strategy with a dopant and sensitizer for solution-processed red TSF-OLEDs with high color purity. Journal of Materials Chemistry C, 2022, 10, 5230-5239.	5.5	7
4	The Intrinsic Thermodynamic Difficulty and a Stepâ€Guided Mechanism for the Epitaxial Growth of Uniform Multilayer MoS <sub>2</sub> with Controllable Thickness. Advanced Materials, 2022, 34, e2201402.	21.0	27
5	Novel ternary exciplex system based on TCTA dendrimer with a new linking type amongst various functional donors. Journal of Materials Science: Materials in Electronics, 2022, 33, 11403-11413.	2.2	6
6	A novel CWPO/H <sub>2</sub> O <sub>2</sub> /VUV synergistic treatment for the degradation of unsymmetrical dimethylhydrazine in wastewater. Environmental Technology (United Kingdom), 2021, 42, 479-491.	2.2	5
7	Constructing host-σ-guest structures to optimize the efficiency of non-doped solution-processed OLEDs. Journal of Materials Chemistry C, 2021, 9, 1221-1227.	5.5	7
8	High electron transfer of TiO2 nanorod@carbon layer supported flower-like WS2 nanosheets for triiodide electrocatalytic reduction. New Journal of Chemistry, 2021, 45, 3387-3391.	2.8	1
9	A biomass-derived, all-day-round solar evaporation platform for harvesting clean water from microplastic pollution. Journal of Materials Chemistry A, 2021, 9, 11013-11024.	10.3	31
10	Yolk-shell silicon/carbon composites prepared from aluminum-silicon alloy as anode materials for lithium-ion batteries. Ionics, 2021, 27, 1939-1948.	2.4	4
11	Stimulus-Responsive Graphene with Periodical Wrinkles on Grooved Microfiber Arrays: Simulation, Programmable Shape-Shifting, and Catalytic Applications. ACS Applied Materials & Interfaces, 2021, 13, 26561-26572.	8.0	5
12	Oxide Nanofibers as Catalysts Toward Energy Conversion and Environmental Protection. Chemical Research in Chinese Universities, 2021, 37, 366-378.	2.6	5
13	Effective Regulation of ZnO Surface Facets for Enhanced Photoluminescence Properties Assisted by Zinc Quaternary Ammonium Salts. ACS Omega, 2021, 6, 17455-17463.	3.5	0
14	One stone two birds: a sinter-resistant TiO <sub>2</sub> nanofiber-based unbroken mat enables PM capture and <i>in situ</i> elimination. Nanoscale, 2021, 13, 20564-20575.	5.6	9
15	Exciplex Formation and Electromer Blocking for Highly Efficient Blue Thermally Activated Delayed Fluorescence OLEDs with Allâ€Solutionâ€Processed Organic Layers. Chemistry - A European Journal, 2020, 26, 3090-3102.	3.3	16
16	Design of Blue Thermally Activated Delayed Fluorescent Emitter with Efficient Exciton Gathering Property for High-Performance Fully Solution-Processed Hybrid White OLEDs. ACS Applied Materials & Interfaces, 2020, 12, 1190-1200.	8.0	38
17	Multidimensional and Binary Micro CuCo <sub>2</sub> O <sub>4</sub> /Nano NiMoO <sub>4</sub> for High-Performance Supercapacitors. ACS Sustainable Chemistry and Engineering, 2020, 8, 1687-1694.	6.7	52
18	Gradient-aligned Au/graphene meshes with confined heat at multiple levels for solar evaporation and anti-gravity catalytic conversion. Journal of Materials Chemistry A, 2020, 8, 16570-16581.	10.3	32

#	Article	IF	CITATIONS
19	Manipulation of the sterically hindering effect to realize AIE and TADF for high-performing nondoped solution-processed OLEDs with extremely low efficiency roll-off. Journal of Materials Chemistry C, 2020, 8, 11850-11859.	5.5	16
20	Succinimide-modified graphite as anode materials for lithium-ion batteries. Electrochimica Acta, 2020, 356, 136858.	5.2	17
21	Stepwise Growth of CuO via Transformation of Cu <sub>2</sub> (OH) <sub>3</sub> Br Intermediate in Aqueous Solution of Long-Alkyl-Chain Copper Salt. Crystal Growth and Design, 2020, 20, 3044-3052.	3.0	2
22	Surfaceâ€Functionalized Graphite as Long Cycle Life Anode Materials for Lithiumâ€Ion Batteries. ChemElectroChem, 2020, 7, 1465-1472.	3.4	32
23	Gradient Vertical Channels within Aerogels Based on N-Doped Graphene Meshes toward Efficient and Salt-Resistant Solar Evaporation. ACS Sustainable Chemistry and Engineering, 2020, 8, 4955-4965.	6.7	36
24	Coupling of Hierarchical Al2O3/TiO2 Nanofibers into 3D Photothermal Aerogels Toward Simultaneous Water Evaporation and Purification. Advanced Fiber Materials, 2020, 2, 93-104.	16.1	81
25	Spatial separation of a TADF sensitizer and fluorescent emitter with a core-dendron system to block the energy loss in deep blue organic light-emitting diodes. Journal of Materials Chemistry C, 2019, 7, 11005-11013.	5.5	30
26	Design of efficient thermally activated delayed fluorescence blue host for high performance solution-processed hybrid white organic light emitting diodes. Chemical Science, 2019, 10, 3054-3064.	7.4	45
27	Surface Engineering of Defective Hematite Nanostructures Coupled by Graphene Sheets with Enhanced Photoelectrochemical Performance. ACS Sustainable Chemistry and Engineering, 2019, 7, 12750-12759.	6.7	6
28	Tuning Electron Transport Direction through the Deposition Sequence of MoS <sub>2</sub> and WS <sub>2</sub> on Fluorineâ€Đoped Tin Oxide for Improved Electrocatalytic Reduction Efficiency. ChemElectroChem, 2019, 6, 2737-2740.	3.4	12
29	Achieving 20% External Quantum Efficiency for Fully Solution-Processed Organic Light-Emitting Diodes Based on Thermally Activated Delayed Fluorescence Dendrimers with Flexible Chains. ACS Applied Materials & Interfaces, 2019, 11, 16737-16748.	8.0	45
30	Chitosan–silica nanoparticles catalyst (M@CS–SiO2) for the degradation of 1,1-dimethylhydrazine. Research on Chemical Intermediates, 2019, 45, 1721-1735.	2.7	16
31	Novel photocatalyst gold nanoparticles with dumbbell-like structure and their superiorly photocatalytic performance for ammonia borane hydrolysis. Nanotechnology, 2018, 29, 165707.	2.6	16
32	Selective Etching of Nâ€Doped Graphene Meshes as Metalâ€Free Catalyst with Tunable Kinetics, High Activity and the Origin of New Catalytic Behaviors. Particle and Particle Systems Characterization, 2018, 35, 1700395.	2.3	12
33	Thermally activated delayed fluorescence dendrimers with exciplex-forming dendrons for low-voltage-driving and power-efficient solution-processed OLEDs. Journal of Materials Chemistry C, 2018, 6, 43-49.	5.5	45
34	Strategy for the Realization of Highly Efficient Solution-Processed All-Fluorescence White OLEDs—Encapsulated Thermally Activated Delayed Fluorescent Yellow Emitters. ACS Applied Materials & Interfaces, 2018, 10, 37335-37344.	8.0	33
35	Core–shell-structured Li <sub>3</sub> V <sub>2</sub> (PO <sub>4</sub> ) <sub>3</sub> –LiVOPO <sub>4</sub> nanocomposites cathode for high-rate and long-life lithium-ion batteries. RSC Advances, 2017, 7, 3101-3107.	3.6	9
36	Self-Host Blue Dendrimer Comprised of Thermally Activated Delayed Fluorescence Core and Bipolar Dendrons for Efficient Solution-Processable Nondoped Electroluminescence. ACS Applied Materials & Interfaces, 2017, 9, 7339-7346.	8.0	86

#	Article	IF	CITATIONS
37	Constructing a Novel Dendron for a Selfâ€Host Blue Emitter with Thermally Activated Delayed Fluorescence: Solutionâ€Processed Nondoped Organic Lightâ€Emitting Diodes with Bipolar Charge Transfer and Stable Color Purity. Chemistry - an Asian Journal, 2017, 12, 216-223.	3.3	15
38	Highly Efficient All-Solution-Processed Fluorescent Organic Light-Emitting Diodes Based on a Novel Self-Host Thermally Activated Delayed Fluorescence Emitter. ACS Applied Materials & Interfaces, 2017, 9, 21900-21908.	8.0	61
39	Graphene sheets manipulated the thermal-stability of ultrasmall Pt nanoparticles supported on porous Fe <sub>2</sub> O <sub>3</sub> nanocrystals against sintering. RSC Advances, 2017, 7, 16379-16386.	3.6	9
40	Unusual Hollow Al <sub>2</sub> O <sub>3</sub> Nanofibers with Loofah-Like Skins: Intriguing Catalyst Supports for Thermal Stabilization of Pt Nanocrystals. ACS Applied Materials & Interfaces, 2017, 9, 21258-21266.	8.0	35
41	Bicolour electroluminescence of 2-(carbazol-9-yl)anthraquinone based on a solution process. Journal of Materials Chemistry C, 2017, 5, 12031-12034.	5.5	34
42	Synthesizing nonstoichiometric Li <sub>3â~'3x</sub> V <sub>2+x</sub> (PO <sub>4</sub> ) <sub>3</sub> /C as cathode materials for high-performance lithium-ion batteries by solid state reaction. RSC Advances, 2017, 7, 32721-32726.	3.6	6
43	A New Insight of the Photothermal Effect on the Highly Efficient Visible-Light-Driven Photocatalytic Performance of Novel-Designed TiO <sub>2</sub> Rambutan-Like Microspheres Decorated by Au Nanorods. Particle and Particle Systems Characterization, 2016, 33, 140-149.	2.3	25
44	Au nano dumbbells catalyzed the cutting of graphene oxide sheets upon plasmon-enhanced reduction. RSC Advances, 2016, 6, 46218-46225.	3.6	10
45	A CTAB-modified S/C nanocomposite cathode for high performance Li–S batteries. RSC Advances, 2016, 6, 92621-92628.	3.6	2
46	Thermally cross-linkable thermally activated delayed fluorescent materials for efficient blue solution-processed organic light-emitting diodes. Journal of Materials Chemistry C, 2016, 4, 8973-8979.	5.5	17
47	Light-driven removal of rhodamine B over SrTiO <sub>3</sub> modified Bi <sub>2</sub> WO <sub>6</sub> composites. RSC Advances, 2016, 6, 83471-83481.	3.6	11
48	Self-host thermally activated delayed fluorescent dendrimers with flexible chains: an effective strategy for non-doped electroluminescent devices based on solution processing. Journal of Materials Chemistry C, 2016, 4, 8810-8816.	5.5	66
49	Electrochemical detection of L-cysteine using a glassy carbon electrode modified with a two-dimensional composite prepared from platinumAand Fe3O4Ananoparticles on reduced graphene oxide. Mikrochimica Acta, 2016, 183, 3221-3228.	5.0	35
50	Novel aggregation-induced emission and thermally activated delayed fluorescence materials based on thianthrene-9,9′,10,10′-tetraoxide derivatives. RSC Advances, 2016, 6, 22137-22143.	3.6	28
51	A novel cyclometalated Ir( <scp>iii</scp> ) complex based luminescence intensity and lifetime sensor for Cu <sup>2+</sup> . RSC Advances, 2016, 6, 16482-16488.	3.6	9
52	Enhanced Electron Affinity and Exciton Confinement in Exciplex-Type Host: Power Efficient Solution-Processed Blue Phosphorescent OLEDs with Low Turn-on Voltage. ACS Applied Materials & Interfaces, 2016, 8, 2010-2016.	8.0	38
53	Bis(phosphine oxide)/triphenylamine based material for solution-processed blue electrofluorescent and green electrophosphorescent devices. RSC Advances, 2015, 5, 48654-48658.	3.6	1
54	Enhanced electron affinity and charge balance property of a bipolar material: highly efficient solution-processed deep blue electrofluorescent and green electrophosphorescent devices. RSC Advances, 2015, 5, 66994-67000.	3.6	5

#	Article	IF	CITATIONS
55	Solution-processed efficient deep-blue fluorescent organic light-emitting diodes based on novel 9,10-diphenyl-anthracene derivatives. RSC Advances, 2015, 5, 29708-29717.	3.6	35
56	Bipolar Host with Multielectron Transport Benzimidazole Units for Low Operating Voltage and High Power Efficiency Solution-Processed Phosphorescent OLEDs. ACS Applied Materials & Interfaces, 2015, 7, 7303-7314.	8.0	60
57	Systematically tuning the ΔE <sub>ST</sub> and charge balance property of bipolar hosts for low operating voltage and high power efficiency solution-processed electrophosphorescent devices. Journal of Materials Chemistry C, 2015, 3, 5004-5016.	5.5	15
58	High Power Efficiency Solution-Processed Blue Phosphorescent Organic Light-Emitting Diodes Using Exciplex-Type Host with a Turn-on Voltage Approaching the Theoretical Limit. ACS Applied Materials & Interfaces, 2015, 7, 25129-25138.	8.0	46
59	Theoretical and experimental investigations on mono-substituted and multi-substituted functional polyhedral oligomeric silsesquioxanes. RSC Advances, 2015, 5, 80339-80345.	3.6	11
60	Ternary Hybrid Material for High-Performance Lithium–Sulfur Battery. Journal of the American Chemical Society, 2015, 137, 12946-12953.	13.7	253
61	Synthesis of MoS <sub>2</sub> /SrTiO <sub>3</sub> composite materials for enhanced photocatalytic activity under UV irradiation. Journal of Materials Chemistry A, 2015, 3, 706-712.	10.3	66
62	A bipolar homoleptic iridium dendrimer composed of diphenylphosphoryl and diphenylamine dendrons for highly efficient non-doped single-layer green PhOLEDs. Journal of Materials Chemistry C, 2015, 3, 981-984.	5.5	18
63	New versatile Pt supports composed of graphene sheets decorated by Fe <sub>2</sub> O <sub>3</sub> nanorods and N-dopants with high activity based on improved metal/support interactions. Journal of Materials Chemistry A, 2015, 3, 125-130.	10.3	25
64	A high triplet energy small molecule based thermally cross-linkable hole-transporting material for solution-processed multilayer blue electrophosphorescent devices. Journal of Materials Chemistry C, 2015, 3, 243-246.	5.5	31
65	Synthesis of MoS <sub>2</sub> /SrZrO <sub>3</sub> heterostructures and their photocatalytic H <sub>2</sub> evolution under UV irradiation. RSC Advances, 2015, 5, 734-739.	3.6	41
66	Binding ofN-substituted pyrrole derivatives to HIV-1 gp41. Journal of Theoretical and Computational Chemistry, 2014, 13, 1450018.	1.8	2
67	Versatile Graphene Quantum Dots with Tunable Nitrogen Doping. Particle and Particle Systems Characterization, 2014, 31, 597-604.	2.3	124
68	Self-host homoleptic green iridium dendrimers based on diphenylamine dendrons for highly efficient single-layer PhOLEDs. Journal of Materials Chemistry C, 2014, 2, 1104-1115.	5.5	40
69	Graphene-wrapped TiO <sub>2</sub> nanofibers with effective interfacial coupling as ultrafast electron transfer bridges in novel photoanodes. Journal of Materials Chemistry A, 2014, 2, 1060-1067.	10.3	75
70	N-doped graphene quantum dots-functionalized titanium dioxide nanofibers and their highly efficient photocurrent response. Journal of Materials Research, 2014, 29, 1408-1416.	2.6	21
71	Luminescent properties and energy transfer of color-tunable Sr3Y2(SiO3)6:Ce3+, Tb3+ phosphors. Journal of Rare Earths, 2014, 32, 933-937.	4.8	17
72	Synthesis, characterization and luminescence properties of SrLa2(MoO4)4:Eu phosphors. Journal of Sol-Gel Science and Technology, 2013, 67, 196-202.	2.4	6

#	Article	IF	CITATIONS
73	Direct electrochemistry of hemoglobin on graphene/Fe3O4 nanocomposite-modified glass carbon electrode and its sensitive detection for hydrogen peroxide. Journal of Solid State Electrochemistry, 2013, 17, 881-887.	2.5	51
74	Growth of single-crystalline rutile TiO2 nanorods on fluorine-doped tin oxide glass for organic–inorganic hybrid solar cells. Journal of Materials Science: Materials in Electronics, 2012, 23, 1657-1663.	2.2	19
75	Star-shaped dendritic hosts based on carbazole moieties for highly efficient blue phosphorescent OLEDs. Journal of Materials Chemistry, 2012, 22, 12016.	6.7	56
76	Nanocables composed of anatase nanofibers wrapped in UV-light reduced graphene oxide and their enhancement of photoinduced electron transfer in photoanodes. Journal of Materials Chemistry, 2011, 21, 18174.	6.7	53
77	Ceramic nanofibers fabricated by electrospinning and their applications in catalysis, environmental science, and energy technology. Polymers for Advanced Technologies, 2011, 22, 326-338.	3.2	307
78	Structural and solvent effects on the spectroscopic properties of 1, 8â€naphthalimide derivatives: A density functional study. International Journal of Quantum Chemistry, 2011, 111, 2234-2241.	2.0	7
79	Computational Characterization of Binding of Small Molecule Inhibitors to HIVâ€1 gp41. Chinese Journal of Chemistry, 2011, 29, 1307-1311.	4.9	1
80	Hierarchical nanostructures of K-birnessite nanoplates on anatase nanofibers and their application for decoloration of dye solution. Journal of Materials Chemistry, 2010, 20, 3157.	6.7	35
81	Quasi-static particle formation of poly(acrylamide/methacrylic acid) in ethanol by using V-65 as initiator. Polymer Chemistry, 2010, 1, 899.	3.9	12
82	Bioelectrochemical response of a choline biosensor fabricated by using polyaniline. Science in China Series B: Chemistry, 2009, 52, 2275-2280.	0.8	2
83	The unmediated choline sensor based on layered double hydroxides in hydrogen peroxide detection mode. Science in China Series B: Chemistry, 2009, 52, 2281-2286.	0.8	1
84	Hydrogen bonding of single acetic acid with water molecules in dilute aqueous solutions. Science in China Series B: Chemistry, 2009, 52, 2219-2225.	0.8	11
85	Behavior of a Layered Double Hydroxide under High Current Density Charge and Discharge Cycles. Journal of Physical Chemistry C, 2009, 113, 7448-7455.	3.1	32
86	Synthesis and characterization of novel two-component conjugated polythiophenes with 3-octyl and 3-isooctylthiophene side chains. Journal of Applied Polymer Science, 2007, 104, 1169-1175.	2.6	10
87	Spatial regulation of electroplex emission via dendritic molecular engineering. Journal of Materials Chemistry C, 0, , .	5.5	2